Water Research X 10 (2021) 100085

Contents lists available at ScienceDirect

Water Research X

journal homepage: https://www.journals.elsevier.com/water-research-x

Enhanced hydraulic cleanability of biofilms developed under a low phosphorus concentration in reverse osmosis membrane systems

Luisa Javier [a], Nadia M. Farhat [a, *], Johannes S. Vrouwenvelder [a, b]

[a] King Abdullah University of Science and Technology (KAUST), Water Desalination and Reuse Center (WDRC), Division of Biological and Environmental Science and Engineering (BESE), Thuwal, 23955-6900, Saudi Arabia
[b] Delft University of Technology, Faculty of Applied Sciences, Department of Biotechnology, Van der Maasweg 9, 2629, HZ Delft, the Netherlands

ARTICLE INFO

Article history:
Received 28 October 2020
Received in revised form
8 December 2020
Accepted 12 December 2020
Available online 14 December 2020

Keywords:
Phosphate limitation
Drinking water production
Biofouling
Biofilm streamers
Seawater desalination

ABSTRACT

A critical problem in seawater reverse osmosis (RO) filtration processes is biofilm accumulation, which reduces system performance and increases energy requirements. As a result, membrane systems need to be periodically cleaned by combining chemical and physical protocols. Nutrient limitation in the feed water is a strategy to control biofilm formation, lengthening stable membrane system performance. However, the cleanability of biofilms developed under various feed water nutrient conditions is not well understood.

This study analyzes the removal efficiency of biofilms grown in membrane fouling simulators (MFSs) supplied with water varying in phosphorus concentrations (3 and 6 μg $P \cdot L^{-1}$ and with constant biodegradable carbon concentration) by applying hydraulic cleaning after a defined 140% increase in the feed channel pressure drop, through increasing the cross-flow velocity from 0.18 m s^{-1} to 0.35 m s^{-1} for 1 h. The two phosphorus concentrations (3 and 6 μg $P \cdot L^{-1}$) simulate the RO feed water without and with the addition of a phosphorus-based antiscalant, respectively, and were chosen based on measurements at a full-scale seawater RO desalination plant. Biomass quantification parameters performed after membrane autopsies such as total cell count, adenosine triphosphate, total organic carbon, and extracellular polymeric substances were used along with feed channel pressure drop measurements to evaluate biofilm removal efficiency. The outlet water during hydraulic cleaning (1 h) was collected and characterized as well. Optical coherence tomography images were taken before and after hydraulic cleaning for visualization of biofilm morphology.

Biofilms grown at 3 μg $P \cdot L^{-1}$ had an enhanced hydraulic cleanability compared to biofilms grown at 6 μg $P \cdot L^{-1}$. The higher detachment for biofilms grown at a lower phosphorus concentration was explained by more soluble polymers in the EPS, resulting in a lower biofilm cohesive and adhesive strength. This study confirms that manipulating the feed water nutrient composition can engineer a biofilm that is easier to remove, shifting research focus towards biofilm engineering and more sustainable cleaning strategies.

1. Introduction

Seawater reverse osmosis (SWRO) membrane systems have emerged in recent decades to overcome the global increase in freshwater demand. A fundamental issue in SWRO filtration processes is the fouling of the membrane. Membrane fouling raises the system's hydraulic resistance and increases energy requirements (Ansari et al., 2020). One of the most challenging types of fouling is biofouling, the excessive growth of a biofilm. A biofilm develops through the attachment and growth of bacterial cells embedded in a produced matrix of extracellular polymeric substances (EPS) (Flemming, 2020). Biofouling negatively impacts the system performance, increasing the feed channel pressure drop, decreasing the flux and salt rejection, and increasing the overall water cost (Siebdrath et al., 2019).

One proposed strategy for biofouling control is limiting biodegradable organic nutrients in the feed water to reduce bacteria's potential to grow (Keinänen et al., 2002; Lehtola et al, 1999, 2001, 2002; Miettinen et al., 1997). In full-scale plants, pretreatment

* Corresponding author.
E-mail address: nadia.farhat@kaust.edu.sa (N.M. Farhat).

https://doi.org/10.1016/j.wroa.2020.100085

processes reduce nutrient concentration and bacterial cell concentration. Feed water pretreatment is done by various processes arranged in different configurations, such as dissolved air flotation, inline coagulation, biologically activated carbon filtration, slow sand filtration, dual media filtration, and ultrafiltration (Abushaban et al., 2019; Farhat et al., 2018). Almost all conventional pretreatment systems used in RO plants utilize low micron range cartridge filter (CF) units as a final protection barrier before the high-pressure pumps of the RO membranes (Farhat et al., 2020). The types of treatment steps applied and sequence of pretreatment processes can vary between plants (there is no standard pretreatment process).

Research has focused on restricting other nutrients, such as phosphorus concentration in the feed water (Javier et al., 2020; Kim et al., 2014; Pinel et al., 2020; Sevcenco et al., 2015; Vrouwenvelder et al., 2010). Although phosphorous limitation has been shown to be effective in delaying biofilm formation and prolonging the system performance, the unintentional addition of phosphorous to the feed water through the dosage of phosphorus-based antiscalants is still performed. Antiscalants are often dosed to the RO feed water to avoid the scaling accumulation on the membrane. It has been previously reported that some antiscalants increase the organic content, and therefore, increase bacterial growth potential (Vrouwenvelder et al., 2000).

Membrane modules are cleaned to remove accumulated fouling and restore system performance, usually when the overall differential pressure drop increases by more than 15% (Singh, 2015). Membrane cleaning is generally done using chemical and physical protocols (Chen et al., 2003). Recent studies focused on advanced physical cleaning methods to reduce the environmental impact and associated cost of chemical cleaning. Several hydraulic cleaning methods are reported in the literature, such as (i) reverse flushing by changing the direction of the flow from the concentrate to the feed side, (ii) reverse module operation where the elements are turned around and the brine seal moved to the other end (Andes et al., 2013), (iii) forward flushing by increasing the cross-flow velocity, (iv) soaking of membranes (McDonald et al., 2004), and (v) gas/liquid two-phase flow cleaning (Wibisono et al., 2014). A previous study showed that among different hydraulic cleaning methods, the reverse operation of modules achieved a higher (15%) feed channel pressure drop recovery (Andes et al., 2013).

Hydrodynamic conditions affect biofilm structure, growth, and detachment (Dreszer et al., 2014; Radu et al., 2012). Previous studies have reported that nutrient load in the feed water affects biofilm morphology and biofilm hydraulic resistance (Desmond et al. 2018c; Farhat et al., 2019). Biofilm morphology plays a vital role in determining the biofilm's mechanical response to hydraulic shear stress (Desmond et al., 2018b). Biofilm streamers are viscoelastic filamentous structures formed by bacteria embedded in strands of EPS (Valiei et al., 2012). Biofilm streamers have caused catastrophic disruption of flow independent of bacterial cell growth (Das and Kumar, 2014; Drescher et al., 2013; Graf von der Schulenburg et al., 2008). Drescher et al. (2013) demonstrated that biofilms attached to the surfaces had little effect on flow, whereas biofilm streamers caused a higher flow disruption. Moreover, a recent study showed biofilm grown under restricted phosphorus conditions, detached by sloughing and peeling off when instantaneously increasing hydraulic shear force (Desmond et al., 2018c). The biofilm detachment was explained by a weaker cohesive strength of the phosphorus-limited biofilm than the non-limited biofilm.

Previously, we demonstrated that biofouling control by phosphorus limitation depends on the assimilable organic carbon concentration (Javier et al., 2020). However, the removal of biofilms developed under various feed water nutrient conditions is not well understood. This study analyzes the removal efficiency of biofilms grown at two phosphorus concentrations (3 and 6 μg $P \cdot L^{-1}$) by applying hydraulic cleaning after a 140% increase in the feed channel pressure drop through increasing the cross-flow velocity from 0.18 m s^{-1} to 0.35 m s^{-1} for 1 h. The same carbon concentration was used for all the experiments to analyze the impact of phosphorus conditions only on biofilm cleanability. The two phosphorus concentrations (3 and 6 μg $P \cdot L^{-1}$) were chosen based on measurements taken at a seawater RO desalination plant (Figure S1 in supplementary material) simulating the RO feed water without and with the addition of a phosphorus-based antiscalant, respectively. Biomass quantification parameters performed after membrane autopsies such as total cell count, adenosine triphosphate, total organic carbon, and extracellular polymeric substances were used along with feed channel pressure drop measurements to evaluate biofilm removal efficiency. The outlet water during hydraulic cleaning (1 h) was collected and characterized as well. The biofilm structure was visualized with Optical Coherence Tomography. To the authors' knowledge, this is the first study that defines a hydraulic cleaning method to evaluate biomass detachment of biofilms grown at different feed water phosphorus conditions, and therefore, propose a more sustainable approach to improve membrane system performance.

2. Materials and methods

2.1. Experimental setup

The feed water used for this study was tap water, produced by reverse osmosis (RO) desalination, supplemented with nutrients (Table 1), to assure an extremely low phosphorus content as a baseline ($\leq$0.3 μg $P \cdot L^{-1}$). The tap water is produced through RO desalination at the King Abdullah University of Science and Technology desalination plant (Thuwal, Jeddah, Saudi Arabia) and distributed to the network with residual chlorine (Belila et al., 2016). The chlorine in the feed water was removed by an activated carbon filter (filter housing model: UPS BB3 [AWF-UPS-3H−20B], cartridge model: sediment-carbon [AC-SC-10-NL]) to protect the membranes. Water was passed through two cartridge filters (pore size 4 μm) to remove particles entering the feed water from the carbon filter.

The experiments were conducted in a lab-scale setup with hydraulics, water characteristics and materials representative of SWRO membrane systems (Farhat et al., 2019). The setup consisted of a feed water pump, a feed flow controller, a pump for dosing the nutrients, a flow cell called a Membrane Fouling Simulator (MFS: Vrouwenvelder et al., 2007), a back-pressure valve (Bronkhorst, Ruurlo, Netherlands) and a differential pressure sensor (Delta bar, PMD75, Endress + Hauser, Switzerland) to monitor the pressure drop over the feed channel. The MFS had inlet and outlet orifices for pressure drop measurements. A reverse osmosis (RO) polyamide membrane sheet with the dimensions of 20 cm × 3.5 cm and a 34 mil (864 μm) thick feed channel spacer, taken from a new commercially available spiral wound membrane element (TW30-4040, DOW FILMTEC, USA) were placed inside the MFS. The feed flow channel height is 0.864 mm, equal to the feed spacer thickness.

2.2. Fouling monitoring by feed channel pressure drop

Earlier work has shown that reverse osmosis biofouling is a feed channel problem (Vrouwenvelder et al., 2009). Pressure drop measurements were recorded as an indicator of system performance of RO biofouling, as feed channel pressure drop was shown to be the first and strongest impacted performance indicator (Siebdrath et al., 2019). Eight fully independent membrane fouling

Table 1
Experimental conditions for the study.

Dosed carbon concentration (μg C·L^{-1}) as glucose	Dosed nitrogen concentration (μg N·L^{-1}) as sodium nitrate	Dosed phosphorus concentration (μg P·L^{-1}) as sodium phosphate	Cleaning procedure
125	25	3	Control
		3	Control
		3	Hydraulic cleaning
		3	Hydraulic cleaning
		6	Control
		6	Control
		6	Hydraulic cleaning
		6	Hydraulic cleaning

simulators were run simultaneously (Table 1), and the figures show the average and standard deviation of duplicate experiments for each scenario. The average initial pressure drop registered in each MFS was 35 ± 5 mbar. For each phosphorus concentration (3 μg P·L^{-1} and 6 μg P·L^{-1}), two MFSs were used as a control, where hydraulic cleaning was not performed. These MFSs were immediately stopped and sampled for biofilm analysis once a feed channel pressure drop increase of 140% (53 mbar) was reached. The pressure drop increase chosen for the MFS simulates the biofouling condition that could be present at the inlet of the lead RO element. This pressure drop increase (140%) over the 0.20 m long MFS can explain a pressure drop increase of 15% over the first stage pressure vessel containing several 1 m long membrane elements is series, as previously reported by Vrouwenvelder et al. (2009, 2008, 2006). Hydraulic cleaning was performed for the remaining two MFSs for each phosphorus condition; once the same pressure drop increase of 53 mbar was achieved. Hydraulic cleaning was performed by increasing the cross-flow velocity from 0.18 m s^{-1} to 0.35 m s^{-1} for 1 h, still in the range of what is commonly applied in practice for hydraulic cleaning procedures. After hydraulic cleaning, the MFSs were stopped for biomass characterization.

2.3. Operating conditions

2.3.1. Operating conditions during biofilm development

The feed water was pumped through the MFS at a flow rate of 17 L h^{-1}, which is equivalent to a linear flow velocity of 0.175 m s^{-1}, representing practical conditions at membrane filtration installations (Bucs et al., 2016). Eight fully independent MFSs (Table 1) were run in parallel in a cross-flow mode at a constant pressure of 2 bar without permeate production. Previous studies showed the same pressure drop increase and biofilm formation in a nanofiltration (NF) installation with and without permeation (Vrouwenvelder et al, 2007a, 2007b). A nutrient stock solution was added to the feed water, containing glucose, sodium nitrate, and sodium phosphate, to enhance biofilm growth in the flow cell. The nutrient stock solution increased the assimilable organic carbon concentration of the feed water by 125 μg C·L^{-1}. The same carbon concentration was used for all the membrane fouling simulators to only analyze the impact of different phosphorus conditions on biofilm removal. The chosen carbon type (glucose) and concentration (125 μg C·L^{-1}) was based on a previous study by Abushaban et al. (2019), where they reported a bacterial growth potential (BGP) of 128 μg C·L^{-1} as glucose for the RO feedwater of a desalination plant performing one cleaning in place (CIP) per year. Previous studies showed that a reasonable carbon to nitrogen ratio (C:N) to promote bacterial growth is 100:20, which was the ratio used for this study (Farhat et al., 2019; Sanawar et al., 2018). The phosphorus concentration in seawater ranges from 3 to 11 μg P·L^{-1}, and after water pretreatment with processes such as coagulation, it may be restricted to values below 1 μg P·L^{-1} (Jacobson et al., 2009; Vrouwenvelder et al., 2010). Figure S1 in supplementary material shows the phosphorous concentrations measurements taken at different stages of the seawater reverse osmosis (SWRO) plant at King Abdullah University of Science and Technology. The phosphorus concentrations for this study, 3 μg P·L^{-1} and 6 μg P·L^{-1}, were selected based on phosphorus measurements which are typically present in seawater (S1) and the RO feed water after the addition of phosphorus-based antiscalants (S3). Chemicals from Sigma Aldrich (Darmstadt, Germany) were purchased in analytical grade. The nutrient stock solution's pH-value was set at 11 by the addition of sodium hydroxide to restrict bacterial growth. The feed water flow rate was high (17.0 L h^{-1}) compared to the dosing flow rate of the nutrient solution (0.03 L h^{-1}). Consequently, the high pH-value of the nutrient solution did not affect the feed water pH of 7.8 (Dreszer et al., 2014). Before nutrient dosage, on day 0, the outlet water from the cross-flow was collected for 1 h to measure adenosine triphosphate, total organic carbon, and total cell count, to use this data as a baseline.

2.3.2. Operating conditions during hydraulic cleaning

Two MFSs for each nutrient condition were hydraulically cleaned once the MFS reached a pressure drop increase of 140% (53 mbar). Cleaning was performed without permeate production; the impact of concentration polarization during cleaning is negligible. In practice, cleaning is done at a much lower feed pressure compared to operation. The cross-flow velocity was increased from 0.18 m s^{-1} to 0.35 m s^{-1} for 1 h and then returned to the original cross-flow conditions (0.18 m s^{-1}) for an additional hour. Once the MFS reached a pressure drop increase of 53 mbar, the outlet water from the cross-flow was collected for 1 h before, during, and after the hydraulic cleaning for characterization purposes (measurements of adenosine triphosphate, total organic carbon, and total cell count). These parameters were used to analyze and quantify the flushed biomass and compared it to what remained on the membrane and feed spacer.

2.4. Biomass quantification and characterization

2.4.1. Total bacterial cell count

At the end of the experiments, the MFSs were stopped and disassembled for biomass characterization. Total bacterial cell counts (TCC) in the biofilm were performed by flow cytometry, following the protocol reported by Neu et al. (2019). Coupons of 4 × 2 cm^2 of the biofouled membrane and spacer were cut from the MFS's inlet and outlet positions. The coupons were then placed in a

capped tube with 40 mL ultrapure water. The samples were vortexed and sonicated for 2 min to detach biomass from the membrane and spacer. A sample of 700 μL was taken from the tube and stained with 7 μL mL^{-1} SYBR Green I (100 ×) diluted from a 10,000 × stock solution (Molecular Probes, Eugene, OR, USA). Next, the samples were incubated in the dark at 35 °C for 10 min. A BD Accuri C6 flow cytometer (BD Accuri Cytometers, Belgium) equipped with a 50 mW laser with a fixed emission wavelength of 488 nm was used for TCC measurements. Fluorescence intensity was collected at FL1 = 533 ± 30 nm, FL3 > 670 nm, with sideward and forward scattered light intensities also obtained. All data were processed with the BD Accuri CFlow® software. Electronic gating was used to select SYBR green-labeled signals to quantify the total bacterial cell count following the procedure described by Hammes and Egli (2005).

2.4.2. Adenosine triphosphate and total organic carbon

Membrane and feed spacer coupons of 4 × 4 cm^2 were retrieved from the MFS inlet and outlet positions to analyze accumulated adenosine triphosphate (ATP) and total organic carbon (TOC). The coupons were placed in a capped tube containing 40 mL of sterile tap water for ATP analysis or ultrapure water for TOC quantification. Next, the tubes were vortexed (for a few seconds) and placed in an ultrasonic water bath (Branson, 5510MTH, output 135 W, 40 kHz) to detach the biomass from membranes and spacers. The sonication procedure (2 min) was repeated until the liquid was homogenous. The water collected from the tubes was used as a sample to determine ATP and TOC concentrations in the biofilms. Samples were measured in duplicate. For ATP measurements, a luminometer (Celsis Advance, Charles River Laboratories, Inc., USA) was used. TOC measurements were performed with a Total Organic Carbon analyzer TOC-VCPH (Shimadzu, Japan) equipped with a high-sensitivity catalyst (High sense TC catalyst; Shimadzu, Japan). A stock solution of potassium hydrogen phthalate (TOC-standard solution ICC-033-5, ULTRA scientific, USA) was diluted with ultrapure water to obtain solutions with carbon concentrations between 0 and 10 mg L^{-1} C, to prepare a calibration curve. The detection limit of the method was about 0.1 mg L^{-1} C.

2.4.3. Extraction and characterization of extracellular polymeric substances (EPS)

EPS was extracted from the biofouled membrane and spacer by cutting a 4 × 4 cm^2 coupon from the MFS and placing it into tubes containing 10 mL of phosphate-buffered saline solution (PBS). The tubes were vortexed for 2 min and sonicated for 5 min to separate the biomass from the membranes and feed spacers. The EPS was extracted following the formaldehyde–NaOH method established by Liu and Fang (2002). In brief, the water collected from the tubes was used as a sample for EPS extraction. A solution of 0.06 mL formaldehyde (36.5%; Sigma-Aldrich, MO, USA) was added to the samples and incubated at 4 °C for 1 h. Next, 4 mL 1 N NaOH was added to the samples and incubated at 4 °C for 3 h, followed by centrifugation for 20 min at 20000×*g*. The supernatant was filtered through a 0.2 μm pore-sized membrane and dialyzed using a 3500 Da dialysis membrane (Thermo Fisher Scientific, USA) for 24 h. Samples were then lyophilized for 48 h and resuspended in 10 mL of ultrapure water. These samples were used to determine the fluorescence excitation-emission matrix (FEEM). The FEEM was measured using a Fluoromax-4 spectrofluorometer (Horiba Scientific, Japan) under excitation of 240–450 nm and emission of 290–600 nm at a speed of 1500 nm min^{-1}, a voltage of 700 V, and a response time of 2 s. FEEM peaks were identified, according to Baghoth et al. (2011). The FEEM plots presented in this study show four main regions: I (humic-like; excitation>280 nm, emission>380 nm), II (protein-like; excitation = 250–280 nm, emission< 380 nm), III (fulvic acid-like; excitation = 220–250 nm, emission> 380 nm), and IV (tyrosine-like; excitation = 220–250 nm, emission = 330–380 nm).

2.5. Optical coherence tomography (OCT)

In-situ imaging of the biofilm in the MFS was visualized using a spectral-domain Optical Coherence Tomography (Thorlabs Ganymede OCT System). The OCT is equipped with a central light source wavelength of 930 nm. The OCT is fitted with a 5 × telecentric scan lens (Thorlabs LSM03BB), providing a maximum scan area of 100 mm^2. OCT uses coherent light to capture the intensity signal of the scattered media in two dimensions (XZ). Two-dimensional images are combined to form three-dimensional (3D) representations (XYZ) in seconds. Six three-dimensional images were taken at the inlet, middle, and outlet positions of each MFS for visualization purposes. Each 3D image consisted of 278 two-dimensional images. Images were taken at a high-resolution frequency of 36 kHz, with a refractive index of 1.33. The images had a length of 5.00 mm and a depth of 1.00 mm with a pixel size in the x-direction of 18.00 μm and a z-direction of 2.13 μm. The images showed in this study were representative from all the images analyzed.

3. Results

3.1. Membrane performance parameter: feed channel pressure drop

This study assessed the hydraulic cleanability of biofilms developed under two phosphorus concentrations (3 μg $P{\cdot}L^{-1}$ and 6 μg $P{\cdot}L^{-1}$) by increasing the cross-flow velocity from 0.18 to 0.35 m s^{-1} for 1 h. We used 140% feed channel pressure drop increase (+53 mbar from the initial value) as a parameter for either stopping the control membrane fouling simulators or for performing the hydraulic cleaning (Figure S2). Biofilms grown under the 3 μg $P{\cdot}L^{-1}$ phosphorus condition took 15 days longer to reach the defined pressure drop (Fig. 1A). Pressure drop recovery after hydraulic cleaning of only 3% was measured for biofilms grown under 6 μg $P{\cdot}L^{-1}$ compared to 60% recovery for biofilms grown under 3 μg $P{\cdot}L^{-1}$ (Fig. 1B). A better recovery in pressure drop was achieved for biofilms grown under a lower phosphorus concentration.

3.2. Biomass characterization

3.2.1. Characterization of the cross-flow outlet water

On day 0 and on the last day of the experiment, we characterized the cross-flow outlet water to quantify total cell count, adenosine triphosphate and total organic carbon before, during and after hydraulic cleaning. The total cell count (TCC) in the cross-flow outlet water was 0.24 × 10^5 cells·mL^{-1} on day 0. An increase in the bacterial cell count in the cross-flow outlet water for both the 3 μg $P{\cdot}L^{-1}$ and 6 μg $P{\cdot}L^{-1}$ was observed when a feed channel pressure drop increase of 53 mbar was reached. The collected cross-flow outlet water before hydraulic cleaning had a total cell count of 0.84 × 10^5 cells·mL^{-1} for the 3 μg $P{\cdot}L^{-1}$, and 0.95 × 10^5 cells·mL^{-1} for the 6 μg $P{\cdot}L^{-1}$ condition. During the hydraulic cleaning, TCC increased to 9.78 and 1.89 × 10^5 cells·mL^{-1}, respectively (Fig. 2A). The increase in the total cell count in the cross-flow outlet water during hydraulic cleaning was higher for the 3 μg $P{\cdot}L^{-1}$ condition, suggesting a better biofilm removal.

Adenosine triphosphate (ATP) in the cross-flow outlet water was 1.25 pg mL^{-1} on day 0. During hydraulic cleaning, a higher ATP concentration was released in the cross-flow outlet water for biofilms grown at 3 μg $P{\cdot}L^{-1}$ phosphorus compared to 6 μg $P{\cdot}L^{-1}$. For the biofilms grown at 3 μg $P{\cdot}L^{-1}$, the ATP concentration was 59.22 pg mL^{-1} before hydraulic cleaning and 871.41 pg mL^{-1} during

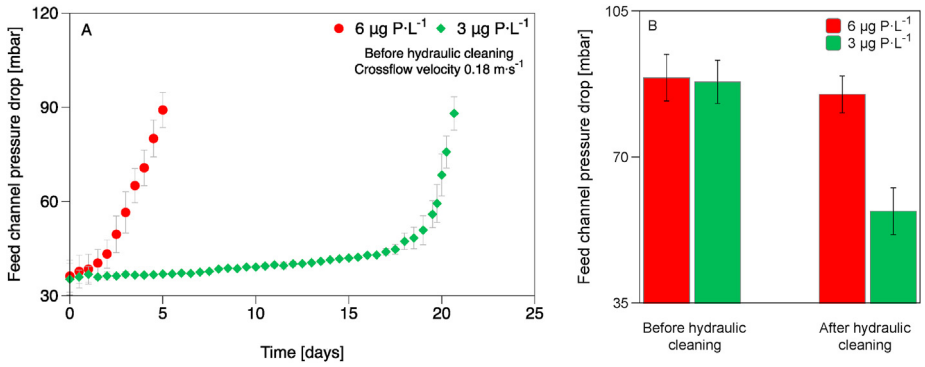

Fig. 1. Feed channel pressure drop plots before and after hydraulic cleaning. (A) Feed channel pressure drop in time over the membrane fouling simulator (MFS) before hydraulic cleaning (n = 4), and (B) feed channel pressure drop before hydraulic cleaning (cross-flow velocity of 0.18 m s^{-1}) and after hydraulic cleaning increasing the cross-flow velocity to 0.35 m s^{-1} for 1 h, for the biofilms grown at 3 µg P·L^{-1} and 6 µg P·L^{-1} in the feed water with a dosed assimilable organic carbon concentration of 125 µg C·L^{-1}. The average of independent duplicate experiments is shown. The MFSs were hydraulically cleaned, stopped, and sampled for biofilm analysis once a feed channel pressure drop increase of 53 mbar was reached.

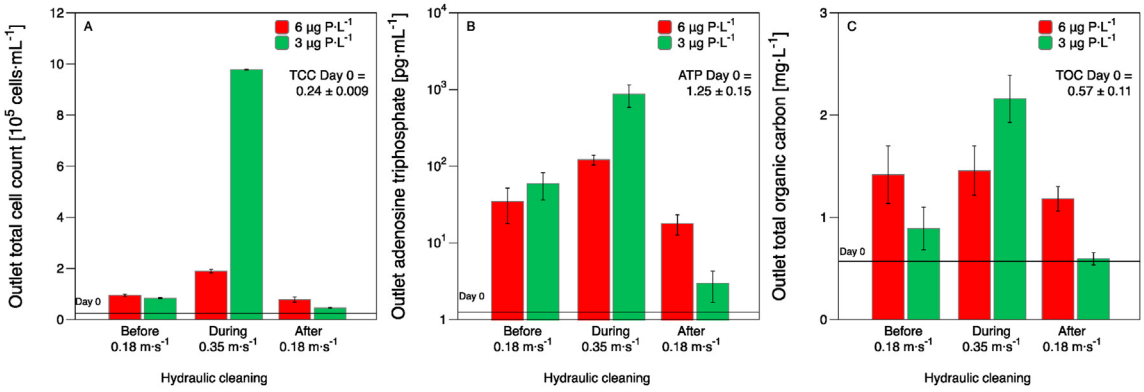

Fig. 2. Cross-flow outlet water characterization before, during, and after hydraulic cleaning. (A) Total cell count (B) adenosine triphosphate, and (C) total organic carbon for the biofilms grown at 3 µg P·L^{-1} and 6 µg P·L^{-1} feed water conditions with a dosed assimilable organic carbon concentration of 125 µg C·L^{-1}, before hydraulic cleaning (cross-flow velocity of 0.18 m s^{-1}), during (cross-flow velocity of 0.35 m s^{-1} for 1 h) and after hydraulic cleaning (cross-flow velocity of 0.18 m s^{-1}). The horizontal black line indicates the baseline at day 0 for each parameter. The average of independent duplicate experiments is shown. The MFSs were hydraulically cleaned, stopped, and sampled for biofilm analysis once a feed channel pressure drop increase of 53 mbar was reached.

hydraulic cleaning, compared to biofilms grown at 6 µg P·L^{-1}, where before and during hydraulic cleaning, the ATP values were 34.85 and 121.74 pg mL^{-1}, respectively (Fig. 2B). The cross-flow outlet water showed a higher amount of adenosine triphosphate during hydraulic cleaning for the 3 µg P·L^{-1} condition, suggesting a better removal of active bacteria.

The total organic carbon (TOC) in the cross-flow outlet water was 0.57 mg L^{-1} on day 0. For biofilms grown at 3 and 6 µg P·L^{-1}, the TOC before hydraulic cleaning was 0.89 and 1.42 mg L^{-1} respectively, and during hydraulic cleaning, the TOC increased to 2.16 and 1.46 mg L^{-1}, respectively. The TOC for the 6 µg P·L^{-1} concentration did not show a significant increase in the cross-flow outlet water during hydraulic cleaning (Fig. 2C). The cross-flow outlet water collected after a pressure drop increase of 140% showed a clearly higher TCC, ATP and TOC values during hydraulic cleaning for biofilms grown at 3 µg P·L^{-1} suggesting better biomass removal.

3.2.2. Biomass characterization on the membrane and spacer

The biomass parameters (total cell count, adenosine triphosphate, and total organic carbon) for the biofouled membrane and spacer lead to the same conclusions as to the cross-flow outlet water. Fig. 3A–B shows the total cell count and adenosine triphosphate of the biofouled membranes and spacers before and after the hydraulic cleaning. The control MFSs, where no hydraulic cleaning was performed, were stopped and autopsied once a feed channel pressure drop increase of 53 mbar was reached. For the control MFSs, the biofilms grown at 6 µg P·L^{-1} showed significantly higher TCC (8.01×10^7 cells·cm^{-2}) and ATP values (88.52×10^3 pg cm^{-2}) compared to biofilms grown at 3 µg P·L^{-1} at the same biodegradable carbon concentration (2.96×10^7 cells·cm^{-2} and 24.44×10^3 pg cm^{-2}, respectively). These results demonstrated that the lower phosphorus concentration restricted bacterial growth in the developed biofilms grown at at 3 µg P·L^{-1} compared to biofilms grown at 6 µg P·L^{-1}. Fig. 3C shows the TOC for biofilms developed at both phosphorus concentrations, 6 and 3 µg P·L^{-1}, which did not show a significant difference at the end of the experiment, 0.071 and 0.067 mg C·cm^{-2}, respectively. The results revealed that biofilms with lower TCC and ATP values before performing hydraulic cleaning had the same pressure drop increase due to the same TOC content.

After 1 h of hydraulic cleaning, two MFSs for each phosphorus concentration were autopsied for biomass characterization by increasing the cross-flow velocity from 0.18 to 0.35 m s^{-1}. The total cell count for the biofilms grown at 3 µg P·L^{-1} showed a 67% reduction after hydraulic cleaning; the TCC went from 2.96 to 0.97×10^7 cells·cm^{-2}, compared with biofilms grown at 6 µg P·L^{-1}, where the TCC value dropped 29% from 8.01 to 5.71×10^7 cells·cm^{-2} (Fig. 3A). Similarly, Fig. 3B demonstrates that the ATP showed the

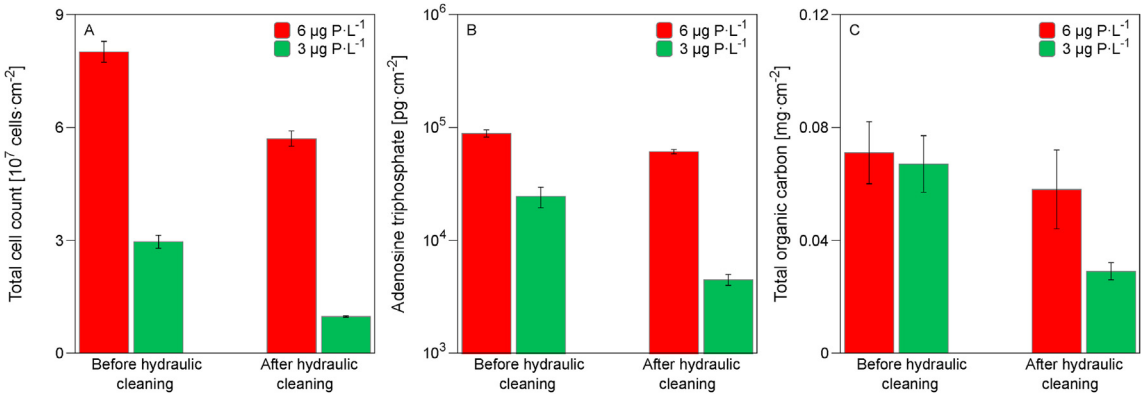

Fig. 3. Biofilm characterization of the biofouled membrane and spacer before and after hydraulic cleaning. (A) Total cell count (B) adenosine triphosphate, and (C) total organic carbon for the biofilms grown at 3 µg P·L^{-1} and 6 µg P·L^{-1} feed water conditions with a dosed assimilable organic carbon concentration of 125 µg C·L^{-1}, before hydraulic cleaning (cross-flow velocity of 0.18 m s^{-1}) and after hydraulic cleaning increasing the cross-flow velocity to 0.35 m s^{-1} for 1 h. The average of independent duplicate experiments is shown. The MFSs were hydraulically cleaned, stopped, and sampled for biofilm analysis once a feed channel pressure drop increase of 53 mbar was reached.

highest reduction (82%) for biofilms developed at 3 µg P·L^{-1} (from 24.44 to 4.48 × 10^3 pg cm^{-2}) compared to biofilms grown at 6 µg P·L^{-1} (from 88.52 to 61.07 × 10^3 pg cm^{-2}). Fig. 3C shows a 55% decrease in TOC for biofilms grown at 3 µg P·L^{-1} (from 0.067 to 0.031 mg cm^{-2}) compared to the 18% TOC decrease for biofilms developed at a higher phosphorus concentration (from 0.071 to 0.058 mg cm^{-2}). In summary, more biofilm biomass, in terms of TCC, ATP and TOC, was removed after hydraulic cleaning for biofilms grown at a lower phosphorus concentration.

At the end of the experiment, extracellular polymeric substances (EPS) were extracted for all the biofouled membranes and spacers to determine organic composition using the fluorescence excitation-emission matrix (FEEM) plots (Fig. 4). Four main regions can be distinguished in the FEEM plot: I (humic-like; excitation>280 nm, emission>380 nm), II (protein-like; excitation = 250–280 nm, emission< 380 nm), III (fulvic acid-like; excitation = 220–250 nm, emission> 380 nm), and IV (tyrosine-like; excitation = 220–250 nm, emission = 330–380 nm). Fig. 4A and C shows the FEEM plots for the biofilm developed at both phosphorus concentrations before hydraulic cleaning. The EPS of both biofilms, 6 and 3 µg P·L^{-1}, showed similar peaks of humic acid-like substances (26,290 and 24,147 counts per second/microAmpere, respectively) and tyrosine like substances (203,069 and 190,120 counts per second/microAmpere, respectively). Biofilms grown at 3 µg P·L^{-1} showed a higher peak in fulvic acid-like substances (158,756 counts per second/microAmpere) compared to biofilms grown at 6 µg P·L^{-1} (104,720 counts per second/microAmpere). A higher fluorescence intensity was shown for biofilms grown at 6 µg P·L^{-1} where a higher peak was observed for protein-like substances (627,976 counts per second/microAmpere) compared to biofilms grown at 3 µg P·L^{-1} (293,873 counts per second/microAmpere). Fig. 4E shows the reduction in fluorescence intensity after hydraulic cleaning for the biofouled membranes and spacers for both conditions. After hydraulic cleaning, the peak for the humic-like substances of the biofilms developed at 6 and 3 µg P·L^{-1}, reduced in 16% and 8%, respectively. A higher reduction was observed in the fluorescence intensity of protein substances for biofilms grown at 3 µg P·L^{-1} (69%) compared to biofilms grown at 6 µg P·L^{-1} (50%), indicating a better protein removal. The removal of fulvic like substances showed a similar result, where the reduction in the peak after hydraulic cleaning was 23% for biofilms grown at 3 µg P·L^{-1}, compared with the reduction of 15% of biofilms grown at 6 µg P·L^{-1}. Tyrosine like substances reduced in a 40% and 48% for biofilms grown at 6 and 3 µg P·L^{-1}, respectively (Fig. 4B and D). In summary before hydraulic cleaning, the TOC was about the same for biofilms grown at both phosphorus concentrations (Fig. 3C). However, Fig. 4 shows that biofilms differing in EPS composition (varying amounts of humic acids, proteins, fulvic acids and tyrosine) had the same pressure drop increase (Fig. 1).

3.3. Biofilm structural properties

The biofilm structure was visualized by optical coherence tomography. Three-dimensional images, each composed of 278 two-dimensional images in the XZ direction, were assessed. The images were taken at the inlet, middle, and outlet positions of each membrane fouling simulator on the last day of the experiments before and after hydraulic cleaning (Fig. 5). Fig. 5E shows an OCT image of a clean membrane and spacer on day 0. Before hydraulic cleaning, for the biofilms grown at 6 µg P·L^{-1} (Fig. 5A), the membranes looked to contain more biofilm, compared to the biofilms grown at 3 µg P·L^{-1} (Fig. 5C). OCT images confirmed biomass characterization results of the biofouled membranes and spacers, where more biomass was removed after hydraulic cleaning for biofilms grown at a lower phosphorus concentration (Fig. 5D), compared to biofilms grown at 6 µg P·L^{-1} (Fig. 5B).

Fig. 5A and C shows the formation of biofilm streamers in both MFSs. These filamentous structures were significantly removed by the hydraulic cleaning for the biofilms grown at 3 µg P·L^{-1} (Fig. 5D), compared to biofilms grown at a higher phosphorus concentration (Fig. 5B). To sum up, for both phosphorus concentrations (3 and 6 µg P·L^{-1}), the biomass quantity and the biofilm streamers caused a detrimental effect on membrane performance, such as pressure drop increase.

Fig. 6 shows a summary of different biomass parameters' reduction after hydraulic cleaning. A slight restoration of 3% in the feed channel pressure drop for biofilms grown at 6 µg P·L^{-1} was accompanied by a reduction of 29% of TCC, 31% of ATP, 18% of TOC, and 50% of proteins. Recovery of 60% in the feed channel pressure drop for biofilms grown at 3 µg P·L^{-1} represented a reduction of 67% of TCC, 82% of ATP, 55% of TOC, and 69% of proteins. The overall results indicate that the biofilms are structurally different due to different nutrient feed water phosphorus concentrations and therefore detach differently in response to changes in flow patterns. Under these circumstances, better removal of active biomass (ATP, TCC) and proteins was achieved by biofilms grown at a lower phosphorus concentration. Therefore, biofilms developed under a low phosphorus concentration demonstrate an enhanced hydraulic cleanability.

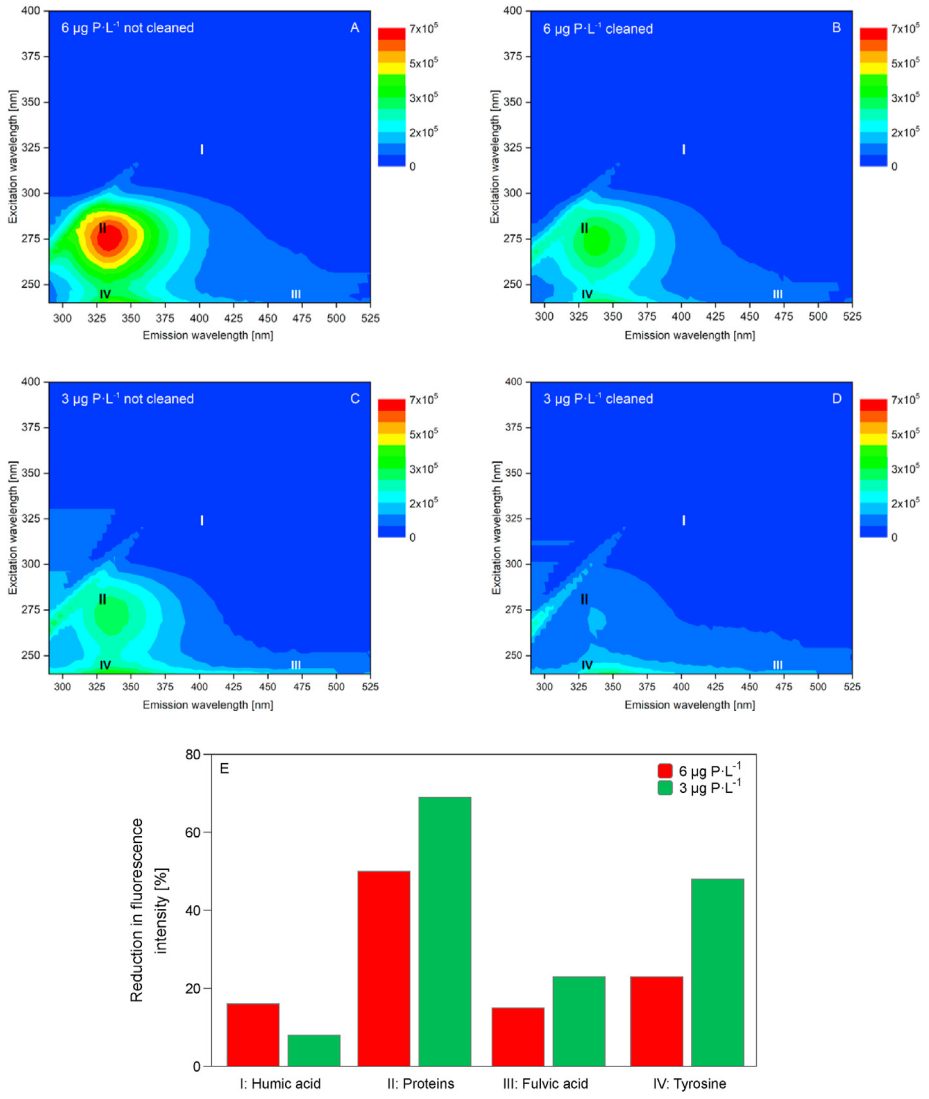

Fig. 4. Fluorescence excitation-emission matrix (FEEM) plots of organic matter extracted from biofouled membrane samples for the biofilms grown under (A) 6 µg P·L^{-1} and (C) 3 µg P·L^{-1} concentration in the feed water. (B) 6 µg P·L^{-1} (D) 3 µg P·L^{-1} show the FEEM plots of organic matter extracted from biofouled membrane samples after hydraulic cleaning. The FEEM plots show the presence of I: Humic-like substances, II: Protein like substances, III: Fulvic acid-like substances, and IV: Tyrosine like substances. (E) Reduction in fluorescence intensity for the four types of substances after hydraulic cleaning by increasing the cross-flow velocity from 0.18 m s^{-1} to 0.35 m s^{-1} for 1 h. The MFSs were hydraulically cleaned, stopped, and sampled for biofilm analysis once a feed channel pressure drop increase of 53 mbar was reached.

4. Discussion

4.1. Biofilms grown at a low phosphorus concentration have an enhanced hydraulic cleanability

Developing effective and reliable biofilm cleaning strategies requires understanding how nutrient composition in the feed water affects biofilm composition. Previous studies have reported various mechanisms to influence biofilm's EPS composition: i) the material of membranes and spacers (Bucs et al., 2017; Miller et al., 2012), ii) the water characteristics (Farhat et al., 2019), and operational conditions of the system (Farhat et al., 2016). Therefore, different EPS composition influence biofilm structural properties and, thus, the biofilm detachment when changes in the cross-flow patterns occur (Desmond et al., 2018a). This study assessed the efficiency of hydraulic cleaning of biofilms grown under two phosphorus concentrations (6 µg P·L^{-1} and 3 µg P·L^{-1}) by increasing the cross-flow velocity from 0.18 m s^{-1} to 0.35 m s^{-1} for 1 h. The results showed a higher pressure drop reduction explained by an enhanced detachment of biofilms grown at a lower phosphorus concentration (Fig. 1B).

We attribute the enhanced detachment of biofilms grown at 3 µg P·L^{-1} to two main factors: i) the composition of EPS and ii) the cohesive strength of phosphorus limiting biofilms. The first factor relates to the composition of the extracellular polymeric substances, thus changing EPS sorption and adhesiveness. Proteins can be involved in hydrophobic interactions resulting in an adsorptive EPS (Lawrence et al., 2007). It has been reported that the adsorptive EPS gives the biofilm sorption characteristics by binding various nutrients, metals, and contaminants, which in turn increases biofilm rigidity (Hobley et al., 2015; Neu and Lawrence, 2010). Moreover, it has been previously shown that phosphate limitation results in the loss of adhesin LapA, an adhesion protein required for biofilm formation (Monds et al., 2007). LapA has been correlated with more permanent associations with surfaces (Petrova and Sauer, 2012). In this study, biofilms grown at a higher phosphorus concentration (6 µg P·L^{-1}) showed 53% higher protein production (Fig. 4), indicating a more rigid and more "sticky" structure,

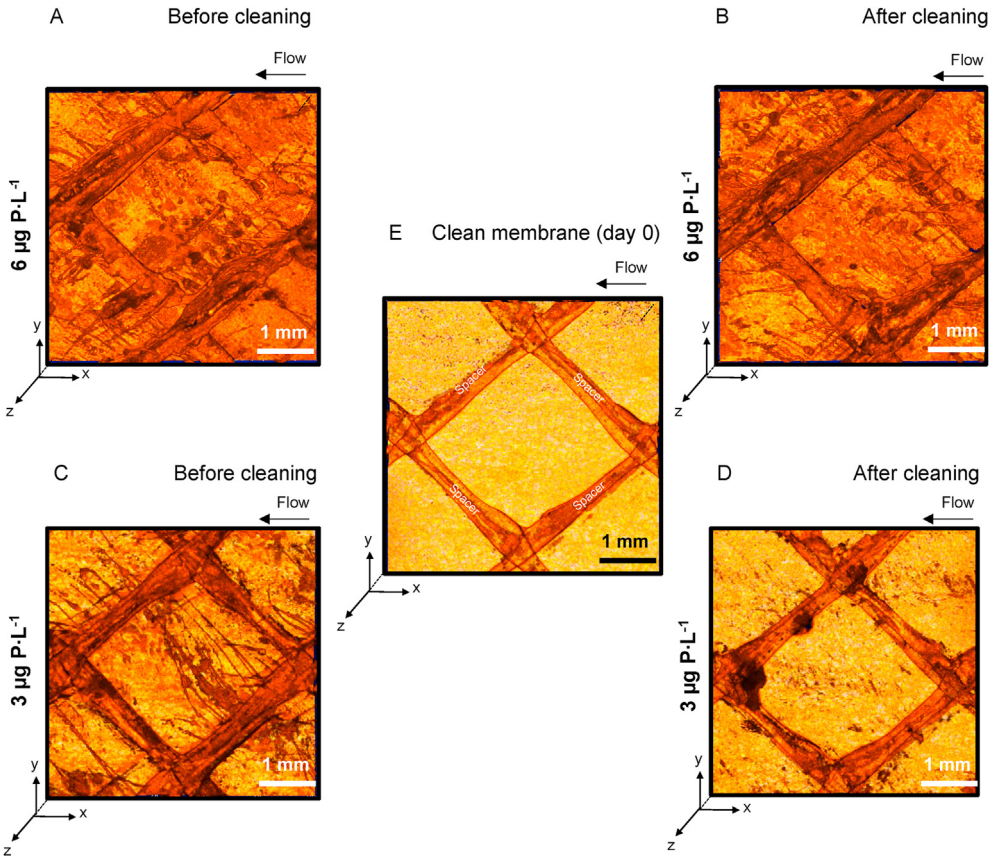

Fig. 5. Three-dimensional visualization (top view) of a clean and biofouled membranes and spacers imaged with optical coherence tomography (OCT). The images (5 mm length) show the biofilms grown under feed water conditions of (A and B) 6 µg $P \cdot L^{-1}$ and (C and D) 3 µg $P \cdot L^{-1}$ with a dosed assimilable organic carbon concentration of 125 µg $C \cdot L^{-1}$, before and after hydraulic cleaning increasing the cross-flow velocity from 0.18 m s^{-1} to 0.35 m s^{-1} for 1 h. E) OCT image of a clean membrane and spacer on day 0 before nutrient dosage. The MFSs were hydraulically cleaned, stopped, and sampled for biofilm analysis once a feed channel pressure drop increase of 53 mbar was reached. Six three-dimensional images were taken at the inlet, middle, and outlet positions of each MFS. The arrow indicates the flow direction.

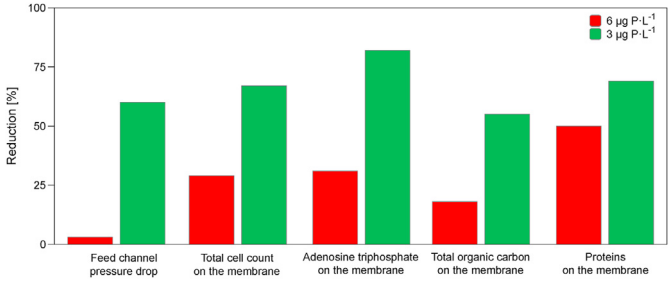

Fig. 6. Membrane performance restoration and biomass removal. The figure shows the percentage of reduction after hydraulic cleaning increasing the cross-flow velocity from 0.18 m s^{-1} to 0.35 m s^{-1} for 1 h, for the biofilms grown at 3 µg $P \cdot L^{-1}$ and 6 µg $P \cdot L^{-1}$ in the feed water with a dosed assimilable organic carbon concentration of 125 µg $C \cdot L^{-1}$. The MFSs were hydraulically cleaned, stopped, and sampled for biofilm analysis once a feed channel pressure drop increase of 53 mbar was reached.

compared to biofilms grown at 3 µg $P \cdot L^{-1}$. An additional finding from this study is the higher amount of fulvic acids (+52%) present for biofilms grown at a lower phosphorus concentration (Fig. 4C), which was reduced after hydraulic cleaning. Humic substances are heterogenic organic constituents found in soils and water. Depending on their solubility, humic substances can be divided into three fractions: humic acids, fulvic acids, and humin (Yee et al., 2006). Fulvic acids are soluble in natural waters independent of the pH. On the contrary, humic acids are insoluble in the water below pH 8 (Davies et al., 1995). Fulvic acids are natural amphiphilic polymers with carboxylic and phenolic-OH groups forming a micelle-like structure (Singh, 2015). It has been suggested that amphiphilic polymers aid bacteria in detaching from interfaces (Neu and Lawrence, 2010). In our study, when the cross-flow was increased for 1 h, the higher presence of fulvic acids in the biofilm grown at a lower phosphorus concentration helped solubilize and detach the biofilm from the membrane and spacer. The combination of lower protein production and more soluble and amphiphilic polymers in the EPS causes the enhanced cleanability of biofilms grown at lower phosphorus concentration.

The second factor relates to the cohesive strength of phosphorus limiting biofilms. EPS composition determines biofilms' mechanical properties, such as cohesive strength, a material's ability to hold itself together under stress (Flemming, 2016; Rowlinson, 2002). Desmond et al. (2018b) showed that biofilms grown under restricted phosphorus conditions sloughed and peeled off from the membrane when increasing the shear stress from 0 to 2 bar pressure in a gravity-driven membrane system. They explained the biofilm detachment by performing a biofilm rheological analysis, where biofilms grown under phosphorus limiting conditions showed a weaker cohesive strength. We confirmed with the OCT images that biofilm structures detached better at a lower phosphorus concentration when increasing the cross-flow velocity (Fig. 5). In agreement with our study, the results confirmed that phosphorus limitation determines the biofilm mechanical properties, such as cohesive strength and the ability of a material to hold itself together under stress.

4.2. Biofilm structural properties play an essential effect on pressure drop increase

Organic compounds in the feed water and hydrodynamic conditions influence biofilm structural properties (Desmond et al., 2018c; Farhat et al., 2019). Some studies have reported the formation of distinct biofilm structures called streamers. These filamentous structures develop in the surface on one or both ends, while the rest is floating in the fluid (Stoodley et al., 2005; Valiei et al., 2012). Biofilm streamers cause significant disruption of the flow, negatively impacting the pressure drop (Das and Kumar, 2014; Graf von der Schulenburg et al., 2008; Valiei et al., 2012). In this study, the higher phosphorus concentration (6 μg $P \cdot L^{-1}$) resulted in biofilm attached to the surfaces and biofilm streamers. On the contrary, at a lower phosphorus concentration, the streamers were the governing biofilm structure (Fig. 5). Both biofilms had a similar total organic carbon (Fig. 3C); however, the phosphate limiting biofilm showed a substantially lower bacterial cell activity (TCC and ATP). This result indicates that regardless of the biomass composition, the biofilm structural properties play a significant role on the pressure drop increase and detachment from membranes and spacers.

4.3. Practical implications

Desalination plants usually dose phosphorus-based antiscalants to control scale formation in the membrane modules, increasing the phosphorus concentration in the feed water (Ali et al., 2015). Antiscalants easily avoid precipitation of soluble salts such as $CaCO_3$ and $CaSO_4$; however, the removal of calcium phosphate is still questionable (Greenberg et al., 2005). Previous research demonstrated that increasing the concentration of phosphorus can lead to the formation of colloidal composites within a very short time of less than seconds, promoting calcium phosphate scaling on the membrane (Dahdal et al., 2016; Pipich et al., 2013). Moreover, it has been previously reported that some antiscalants can increase the assimilable organic content in the feed water, and therefore increase the biofouling potential (Vrouwenvelder et al., 2000). Our study recommends a low-cost optimization strategy for reverse osmosis desalination plants by lowering or avoiding the increase of the phosphorus concentration in the feed water by adding different chemicals (antiscalants, acids, biocides) to develop a biofilm with enhanced hydraulic cleanability. The phosphates added to the antiscalants get concentrated in the brine and act as a nutrient for algae promoting eutrophication when brine is discharged into the sea generating environmental problems (El Din et al., 1994; Popov et al., 2017). Besides the environmental advantages of dosing phosphorus-free antiscalants, if phosphorus limitation is combined with carbon restriction after feed water pretreatment, the approach could delay biofilm formation prolonging the system performance (Javier et al., 2020). Our recommendation to lower the phosphorus and carbon concentration in the feed water and periodic hydraulic cleaning anticipate a sustainable method to extend system performance, while maintaining water production and, therefore, reducing the overall water cost.

4.4. Future research

Biofouling control strategies have focused mainly on eradicating biofilm development (Araújo et al., 2012a; Kim and Park, 2016). This study proves that biofilm engineering, e.g., manipulating the feed water nutrient composition, would enable improved biofilm management strategies. In that sense, it will be possible to engineer, control, and manage biofilms that are easier to be cleaned by solubilization and removal. This study evaluated the detachment of biofilm grown at two phosphorus concentrations after performing a hydraulic cleaning. The characterization of the EPS on the membrane and the biomass quantification of the outlet water when increasing the cross-flow velocity could be used to determine the removal potential of biofilms grown at different nutrient conditions to changes in the cross-flow pattern. Future research should focus on testing (i) different nutrient conditions and (ii) permeate conditions and their effect on biofilm detachment. This data could be used to customize and design more effective cleaning protocols for better biofilm removal, such as (i) the proper selection of hydraulic cleaning methods (backflush, forward flush, bubbles, gas/liquid two-phase flow cleaning), (ii) the effect of hydraulic cleaning combined with chemical cleaning along with membrane and spacer modification for biofouling control (Araújo et al., 2012b; Bucs et al., 2017), and (iii) the optimization of operational parameters during cleaning procedures (Chen et al., 2003). It has been shown that cleaning-in-place (CIP) efficiency is lower for full-scale RO than lab-scale MFS (Jafari et al., 2020). Therefore, further studies should also be performed in full-scale installations by lowering the phosphorus concentration in the feed water to validate the efficiency of cleaning strategies.

5. Conclusions

This study analyzed the effect of hydraulic cleaning by increasing the cross-flow velocity from 0.18 m s^{-1} to 0.35 m s^{-1} for 1 h on biofilm grown at two phosphorus concentrations (3 μg $P \cdot L^{-1}$ and 6 μg $P \cdot L^{-1}$) with the same biodegradable organic carbon content. Feed channel pressure drop measurements and the characterization of the MFS cross-flow outlet water and biomass on the membrane and spacer were used as an indicator to analyze system performance and hydraulic cleaning efficiency. The membrane fouling simulators were hydraulically cleaned, stopped, and sampled for biofilm analysis (TCC, ATP, TOC and EPS characterization) once a feed channel pressure drop increase of 53 mbar was reached (+140% from its initial value). The conclusions of this study can be summarized by:

(i) Biofilms grown at 3 μg $P \cdot L^{-1}$ have a higher hydraulic cleanability compared to biofilms grown a 6 μg $P \cdot L^{-1}$. The higher detachment for biofilms grown at a lower phosphorus concentration is explained by fewer proteins and more soluble polymers in the EPS, translating in a lower biofilm cohesive and adhesive strength.
(ii) Different biomass composition (in terms of ATP, TCC and EPS components) can have the same detrimental effect on pressure drop increase, explained by the biofilm's structural arrangement in the flow channel (biofilm streamers).
(iii) The manipulation of nutrient composition in the feed water could develop biofilms that are easier to be removed by hydraulic cleaning methods.
(iv) The use of phosphorus-based antiscalants increases the phosphorus concentration in the feed water, thereby producing a biofilm with higher cohesive strength and subsequently, reducing the biofilm hydraulic cleanability.
(v) The hydraulic cleaning technique proposed in this study could be used to analyze the detachment of biofilms grown at different nutrient composition.

Declaration of competing interest

The authors declare that they have no known competing financial interests or personal relationships that could have appeared to influence the work reported in this paper.

Acknowledgments

The research reported in this publication was supported by funding from King Abdullah University of Science and Technology (KAUST).

Appendix A. Supplementary data

Supplementary data to this article can be found online at https://doi.org/10.1016/j.wroa.2020.100085.

References

Abushaban, A., Salinas-Rodriguez, S.G., Dhakal, N., Schippers, J.C., Kennedy, M.D., 2019. Assessing pretreatment and seawater reverse osmosis performance using an ATP-based bacterial growth potential method. Desalination 467, 210–218.
Ali, S.A., Kazi, I.W., Rahman, F., 2015. Synthesis and evaluation of phosphate-free antiscalants to control CaSO4·2H2O scale formation in reverse osmosis desalination plants. Desalination 357, 36–44.
Andes, K., Bartels, C.R., Liu, E., Sheehy Presenter, N., Manager -Hydranautics, D., 2013. Methods for Enhanced Cleaning of Fouled RO Elements.
Ansari, A., Peña-Bahamonde, J., Fanourakis, S.K., Hu, Y., Rodrigues, D.F., 2020. Microbially-induced mineral scaling in desalination conditions: mechanisms and effects of commercial antiscalants. Water Res. 179, 115863.
Araújo, P.A., Kruithof, J.C., Van Loosdrecht, M.C.M., Vrouwenvelder, J.S., 2012a. The potential of standard and modified feed spacers for biofouling control. J. Membr. Sci. 403–404, 58–70.
Araújo, P.A., Miller, D.J., Correia, P.B., Van Loosdrecht, M.C.M., Kruithof, J.C., Freeman, B.D., Paul, D.R., Vrouwenvelder, J.S., 2012b. Impact of feed spacer and membrane modification by hydrophilic, bactericidal and biocidal coating on biofouling control. Desalination 295, 1–10.
Baghoth, S.A., Sharma, S.K., Amy, G.L., 2011. Tracking natural organic matter (NOM) in a drinking water treatment plant using fluorescence excitation–emission matrices and PARAFAC. Water Res. 45, 797–809.
Belila, A., El-Chakhtoura, J., Otaibi, N., Muyzer, G., Gonzalez-Gil, G., Saikaly, P.E., van Loosdrecht, M.C.M., Vrouwenvelder, J.S., 2016. Bacterial community structure and variation in a full-scale seawater desalination plant for drinking water production. Water Res. 94, 62–72.
Bucs, S.S., Farhat, N., Siddiqui, A., Valladares Linares, R., Radu, A., Kruithof, J.C., Vrouwenvelder, J.S., 2016. Development of a setup to enable stable and accurate flow conditions for membrane biofouling studies. Desalin. Water Treat. 57, 12893–12901.
Bucs, S.S., Linares, R.V., Farhat, N., Matin, A., Khan, Z., van Loosdrecht, M.C.M., Yang, R., Wang, M., Gleason, K.K., Kruithof, J.C., Vrouwenvelder, J.S., 2017. Coating of reverse osmosis membranes with amphiphilic copolymers for biofouling control. Desalin. Water Treat. 68, 1–11.
Chen, J.P., Kim, S.L., Ting, Y.P., 2003. Optimization of membrane physical and chemical cleaning by a statistically designed approach. J. Membr. Sci. 219, 27–45.
Dahdal, Y.N., Pipich, V., Rapaport, H., Oren, Y., Kasher, R., Schwahn, D., 2016. Small-angle neutron scattering studies of alginate as biomineralizing agent and scale initiator. Polymer 85, 77–88.
Das, S., Kumar, A., 2014. Formation and post-formation dynamics of bacterial biofilm streamers as highly viscous liquid jets. Sci. Rep. 4, 1–6.
Davies, G., Ghabbour, E.A., Jansen, S., Varnum, J., 1995. Humic acids are versatile natural polymers. Polymers and Other Advanced Materials. Springer US, pp. 677–685.
Desmond, P., Best, J.P., Morgenroth, E., Derlon, N., 2018a. Linking composition of extracellular polymeric substances (EPS) to the physical structure and hydraulic resistance of membrane bio fi lms. Water Res. 132, 211–221.
Desmond, P., Böni, L., Fischer, P., Morgenroth, E., Derlon, N., 2018b. Stratification in the physical structure and cohesion of membrane biofilms —implications for hydraulic resistance. J. Membr. Sci.
Desmond, P., Morgenroth, E., Derlon, N., 2018c. Physical structure determines compression of membrane biofilms during Gravity Driven Membrane (GDM) ultrafiltration. Water Res. 143, 539–549.
Drescher, K., Shen, Y., Bassler, B.L., Stone, H.A., 2013. Biofilm streamers cause catastrophic disruption of flow with consequences for environmental and medical systems. Proc. Natl. Acad. Sci. U.S.A. 110, 4345–4350.
Dreszer, C., Flemming, H.-C., Zwijnenburg, A., Kruithof, J.C., Vrouwenvelder, J.S., 2014. Impact of biofilm accumulation on transmembrane and feed channel pressure drop: effects of crossflow velocity, feed spacer and biodegradable nutrient. Water Res. 50, 200–211.
El Din, A.M.S., Aziz, S., Makkawi, B., 1994. Electricity and water production in the Emirate of Abu Dhabi and its impact on the environment. Desalination 97, 373–388.
Farhat, N., Hammes, F., Prest, E., Vrouwenvelder, J., 2018. A uniform bacterial growth potential assay for different water types. Water Res. 142, 227–235.
Farhat, N.M., Christodoulou, C., Placotas, P., Blankert, B., Sallangos, O., Vrouwenvelder, J.S., 2020. Cartridge filter selection and replacement: optimization of produced water quantity, quality, and cost. Desalination 473, 114172.
Farhat, N.M., Javier, L., Van Loosdrecht, M.C.M., Kruithof, J.C., Vrouwenvelder, J.S., 2019. Role of feed water biodegradable substrate concentration on biofouling: biofilm characteristics, membrane performance and cleanability. Water Res. 150, 1–11.
Farhat, N.M., Staal, M., Bucs, S.S., Van Loosdrecht, M.C.M., Vrouwenvelder, J.S., 2016. Spatial heterogeneity of biofouling under different cross-flow velocities in reverse osmosis membrane systems. J. Membr. Sci. 520, 964–971.
Flemming, H.-C., 2016. EPS—then and now. Microorganisms 4, 41.
Flemming, H.C., 2020. Biofouling and me: my Stockholm syndrome with biofilms. Water Res.
Graf von der Schulenburg, D.A., Vrouwenvelder, J.S., Creber, S.A., van Loosdrecht, M.C.M., Johns, M.L., 2008. Nuclear magnetic resonance microscopy studies of membrane biofouling. J. Membr. Sci. 323, 37–44.
Greenberg, G., Hasson, D., Semiat, R., 2005. Limits of RO recovery imposed by calcium phosphate precipitation. Desalination 183, 273–288.
Hammes, F.A., Egli, T., 2005. New method for assimilable organic carbon determination using flow-cytometric enumeration and a natural microbial consortium as inoculum. Environ. Sci. Technol. 39, 3289–3294.
Hobley, L., Harkins, C., Macphee, C.E., Stanley-Wall, N.R., 2015. Giving structure to the biofilm matrix: an overview of individual strategies and emerging common themes. FEMS Microbiol. Rev. 15, 649–669.
Jacobson, J.D., Kennedy, M.D., Amy, G., Schippers, J.C., 2009. Phosphate limitation in reverse osmosis: an option to control biofouling? Desalin. Water Treat. 5, 198–206.
Jafari, M., D'haese, A., Zlopasa, J., Cornelissen, E.R., Vrouwenvelder, J.S., Verbeken, K., Verliefde, A., van Loosdrecht, M.C.M., Picioreanu, C., 2020. A comparison between chemical cleaning efficiency in lab-scale and full-scale reverse osmosis membranes: role of extracellular polymeric substances (EPS). J. Membr. Sci. 609, 118189.
Javier, L., Farhat, N.M., Desmond, P., Linares, R.V., Bucs, S., Kruithof, J.C., Vrouwenvelder, J.S., 2020. Biofouling control by phosphorus limitation strongly depends on the assimilable organic carbon concentration. Water Res. 183, 116051.
Keinänen, M.M., Korhonen, L.K., Lehtola, M.J., Miettinen, I.T., Martikainen, P.J., Vartiainen, T., Suutari, M.H., 2002. The microbial community structure of drinking water biofilms can be affected by phosphorus availability. Appl. Environ. Microbiol. 68, 434–439.
Kim, C.M., Kim, S.J., Kim, L.H., Shin, M.S., Yu, H.W., Kim, I.S., 2014. Effects of phosphate limitation in feed water on biofouling in forward osmosis (FO) process. Desalination 349, 51–59.
Kim, T.S., Park, H.D., 2016. Lauroyl arginate ethyl: an effective antibiofouling agent applicable for reverse osmosis processes producing potable water. J. Membr. Sci. 507, 24–33.
Lawrence, J.R., Swerhone, G.D.W., Kuhlicke, U., Neu, T.R., 2007. In situ evidence for microdomains in the polymer matrix of bacterial microcolonies. Can. J. Microbiol. 53, 450–458.
Lehtola, M.J., Miettinen, I.T., Vartiainen, T., Martikainen, P.J., 2002. Changes in content of microbially available phosphorus, assimilable organic carbon and microbial growth potential during drinking water treatment processes. Water Res. 36, 3681–3690.
Lehtola, M.J., Miettinen, I.T., Vartiainen, T., Martikainen, P.J., 1999. A New Sensitive Bioassay for Determination of Microbially Available Phosphorus in Water, vol. 65, pp. 5–8.
Lehtola, M.J., Miettinen, I.T., Vartiainen, T., Myllykangas, T., Martikainen, P.J., 2001. Microbially available organic carbon, phosphorus, and microbial growth in ozonated drinking water. Water Res. 35, 1635–1640.
Liu, H., Fang, H.H.P., 2002. Extraction of extracellular polymeric substances (EPS) of sludges. J. Biotechnol. 95, 249–256.
McDonald, J., Christophersen, D., Howell, C., 2004. Reduce membrane fouling with good CIP procedures. Ultrapure Water 21, 17–20.
Miettinen, I.T., Vartiainen, T., Martikainen, P.J., 1997. Phosphorus and bacterial growth in drinking water. Appl. Environ. Microbiol. 63.
Miller, D.J., Araújo, P.A., Correia, P.B., Ramsey, M.M., Kruithof, J.C., van Loosdrecht, M.C.M., Freeman, B.D., Paul, D.R., Whiteley, M., Vrouwenvelder, J.S., 2012. Short-term adhesion and long-term biofouling testing of polydopamine and poly(ethylene glycol) surface modifications of membranes and feed spacers for biofouling control. Water Res. 46, 3737–3753.
Monds, R.D., Newell, P.D., Gross, R.H., O'Toole, G.A., 2007. Phosphate-dependent modulation of c-di-GMP levels regulates Pseudomonas fluorescens Pf0-1 biofilm formation by controlling secretion of the adhesin LapA. Mol. Microbiol. 63, 656–679.
Neu, L., Proctor, C.R., Walser, J.-C., Hammes, F., 2019. Small-scale heterogeneity in drinking water biofilms. Front. Microbiol. 10, 2446.
Neu, T.R., Lawrence, J.R., 2010. Extracellular polymeric substances in microbial biofilms. Microbial Glycobiology. Elsevier Inc., pp. 733–758
Petrova, O.E., Sauer, K., 2012. Sticky situations: key components that control bacterial surface attachment. J. Bacteriol.
Pinel, I.S.M., Kim, L.H., Proença Borges, V.R., Farhat, N.M., Witkamp, G.J., van Loosdrecht, M.C.M., Vrouwenvelder, J.S., 2020. Effect of phosphate availability on biofilm formation in cooling towers. Biofouling 36, 800–815.
Pipich, V., Dahdal, Y., Rapaport, H., Kasher, R., Oren, Y., Schwahn, D., 2013. Effects of Biological Molecules on Calcium Mineral Formation Associated with Wastewater Desalination as Assessed Using Small-Angle Neutron Scattering.
Popov, K., Boglovskiy, A., Guseva, O., Larchenko, V., Rudakova, G., 2017. A comparative study of phosphonate and phosphorus-free antiscalant

efficiency by static and dynamic methods. Do we have reliable tools for an adequate reagent selection? Recent Adv. Petrochemical Sci. 1.
Radu, A.I., Vrouwenvelder, J.S., van Loosdrecht, M.C.M., Picioreanu, C., 2012. Effect of flow velocity, substrate concentration and hydraulic cleaning on biofouling of reverse osmosis feed channels. Chem. Eng. J. 188, 30–39.
Rowlinson, J.S., 2002. Cohesion. Cambridge University Press.
Sanawar, H., Pinel, I., Farhat, N.M., Bucs, S.S., Zlopasa, J., Kruithof, J.C., Witkamp, G.J., van Loosdrecht, M.C.M., Vrouwenvelder, J.S., 2018. Enhanced biofilm solubilization by urea in reverse osmosis membrane systems. Water Res. X 1, 100004.
Sevcenco, A.M., Paravidino, M., Vrouwenvelder, J.S., Wolterbeek, H.T., van Loosdrecht, M.C.M., Hagen, W.R., 2015. Phosphate and arsenate removal efficiency by thermostable ferritin enzyme from Pyrococcus furiosus using radioisotopes. Water Res. 76, 181–186.
Siebdrath, N., Farhat, N., Ding, W., Kruithof, J., Vrouwenvelder, J.S., 2019. Impact of membrane biofouling in the sequential development of performance indicators: feed channel pressure drop, permeability, and salt rejection. J. Membr. Sci. 585, 199–207.
Singh, R., 2015. Water and membrane treatment. Membrane Technology and Engineering for Water Purification. Elsevier, pp. 81–178.
Stoodley, P., Dodds, I., De Beer, D., Scott, H.L., Boyle, J.D., 2005. Flowing biofilms as a transport mechanism for biomass through porous media under laminar and turbulent conditions in a laboratory reactor system. Biofouling 21, 161–168.
Valiei, A., Kumar, A., Mukherjee, P.P., Liu, Y., Thundat, T., 2012. A web of streamers: biofilm formation in a porous microfluidic device. Lab Chip 12, 5133–5137.
Vrouwenvelder, J.S., Bakker, S.M., Cauchard, M., Le Grand, R., Apacandié, M., Idrissi, M., Lagrave, S., Wessels, L.P., van Paassen, J.A.M., Kruithof, J.C., van Loosdrecht, M.C.M., 2007a. The membrane fouling simulator: a suitable tool for prediction and characterisation of membrane fouling. Water Sci. Technol. 55, 197–205.
Vrouwenvelder, J.S., Bakker, S.M., Wessels, L.P., van Paassen, J.A.M., 2007b. The Membrane Fouling Simulator as a new tool for biofouling control of spiral-wound membranes. Desalination 204, 170–174.
Vrouwenvelder, J.S., Beyer, F., Dahmani, K., Hasan, N., Galjaard, G., Kruithof, J.C., Van Loosdrecht, M.C.M., 2010. Phosphate limitation to control biofouling. Water Res. 44, 3454–3466.
Vrouwenvelder, J.S., Hinrichs, C., Van der Meer, W.G.J., Van Loosdrecht, M.C.M., Kruithof, J.C., 2009. Pressure drop increase by biofilm accumulation in spiral wound RO and NF membrane systems: role of substrate concentration, flow velocity, substrate load and flow direction. Biofouling 25, 543–555.
Vrouwenvelder, J.S., Manolarakis, S.A., van der Hoek, J.P., van Paassen, J.A.M., van der Meer, W.G.J., van Agtmaal, J.M.C., Prummel, H.D.M., Kruithof, J.C., van Loosdrecht, M.C.M., 2008. Quantitative biofouling diagnosis in full scale nanofiltration and reverse osmosis installations. Water Res. 42, 4856–4868.
Vrouwenvelder, J.S., Manolarakis, S.A., Veenendaal, H.R., Van Der Kooij, D., 2000. Biofouling potential of chemicals used for scale control in RO and NF membranes. Desalination 132, 1–10.
Vrouwenvelder, J.S., van Paassen, J.A.M., Wessels, L.P., van Dam, A.F., Bakker, S.M., 2006. The Membrane Fouling Simulator: a practical tool for fouling prediction and control. J. Membr. Sci. 281, 316–324.
Wibisono, Y., Cornelissen, E.R., Kemperman, A.J.B., Van Der Meer, W.G.J., Nijmeijer, K., 2014. Two-phase flow in membrane processes: a technology with a future. J. Membr. Sci.
Yee, M.M., Miyajima, T., Takisawa, N., 2006. Evaluation of amphiphilic properties of fulvic acid and humic acid by alkylpyridinium binding study. Colloids Surfaces A Physicochem. Eng. Asp. 272, 182–188.